Automated Multi-Sensor Telemetry Filtering and Hardware-in-the-Loop Ground-Truth Acquisition for Mechatronic Actuators

Raveendra Kumar Doddi, Sai Krishna Varma, Karthik Reddy
Department of Mechanical and Mechatronics Systems Engineering / Applied Control & Telemetry Laboratory
Email: dodik8700@gmail.com

***Abstract*—**System identification and empirical modeling of precision mechatronic actuators require high-fidelity ground-truth trajectory logs free from electromagnetic interference (EMI), structural frame resonance, and asynchronous clock jitter. In practical laboratory testbeds combining micro-electromechanical inertial sensors (MEMS IMUs), magnetic rotary encoders, and shunt current monitors, raw telemetry streams exhibit severe non-Gaussian spikes and mechanical deadband distortions that corrupt downstream parameter estimation and data-driven regression models. This paper presents an automated hardware-in-the-loop (HIL) telemetry acquisition and ground-truth curation framework designed for single- and multi-axis electromechanical stages. The architecture integrates deterministic 1 kHz interrupt-driven sampling on an ARM Cortex-M4 microcontroller with a two-stage offline ground-truth pipeline: (i) an Extended Kalman Filter (EKF) coupled with a chi-square Mahalanobis innovation gate to reject transient PWM switching spikes, and (ii) zero-phase Savitzky-Golay kinematic differentiation paired with an analytical leadscrew/belt backlash hysteresis compensator. Experimental validation across 4,200 motion trajectories on a NEMA-17 belt-driven linear gantry and a geared rotary actuator demonstrates that the proposed pipeline reduces velocity ground-truth root-mean-square error (RMSE) by 83.6% against an optical linear glass scale reference, lowers Allan deviation bias instability by a factor of 4.4x, and automatically isolates 99.1% of corrupted telemetry frames prior to dataset archiving.

Keywords*—Hardware-in-the-Loop (HIL), Ground-Truth Data Acquisition, Extended Kalman Filter, Mahalanobis Outlier Gating, Backlash Hysteresis Compensation, Allan Variance, Mechatronic Telemetry.*

1. INTRODUCTION

Empirical characterization of electromechanical actuators—including hybrid stepper linear stages, brushless DC (BLDC) servo drives, and robotic serial linkages—relies heavily on the quality of recorded experimental sensor logs [1], [2]. As data-driven system identification and statistical learning techniques gain adoption in condition monitoring and precision motion control, the predictive accuracy of fitted models is fundamentally bounded by the fidelity of the underlying ground-truth calibration dataset [3], [4]. When training or validating dynamic friction, backlash, or thermal derating models, unmitigated sensor corruption acts as structured label noise that biases least-squares and neural network estimators alike.

In low-cost and mid-range laboratory instrumentation, capturing clean ground-truth telemetry remains challenging due to three concurrent hardware phenomena. First, pulse-width modulation (PWM) switching in H-bridge and three-phase MOSFET inverters (typically operating at 16–24 kHz) injects high-frequency common-mode voltage spikes into adjacent Serial Peripheral Interface (SPI) and Inter-Integrated Circuit (I2C) sensor buses [5]. Second, rigid mounting of MEMS accelerometers and gyroscopes onto aluminum extrusion frames couples structural resonance modes directly into kinematic measurements [6]. Third, mechanical transmission elements such as trapezoidal leadscrews, GT2 synchronous timing belts, and planetary gearheads introduce direction-dependent deadband (backlash hysteresis) between motor-side rotary encoders and load-side linear displacement [7], [8].

Conventional laboratory workflows rely on manual post-experiment visual inspection of oscilloscope or CSV traces to discard corrupted runs, followed by causal low-pass Butterworth filtering. However, manual curation does not scale to multi-thousand-trajectory endurance datasets, and causal infinite-impulse-response (IIR) filters introduce frequency-dependent phase lag that distorts velocity reversal instants critical for Coulomb friction and deadband identification [9].

To address these limitations, this paper develops an automated multi-sensor telemetry acquisition and offline ground-truth curation pipeline for mechatronic testbeds. The specific contributions of this work are threefold: (1) a deterministic hardware synchronization scheme on an STM32F407 microcontroller that aligns rotary encoder, MEMS IMU, and current-shunt channels within a 12 us sampling skew window; (2) a statistically gated Extended Kalman Filter (EKF) combined with zero-phase Savitzky-Golay polynomial smoothing that strips EMI spikes and structural vibration without introducing phase delay; and (3) an automated dataset quality-control (QC) audit that characterizes bidirectional backlash hysteresis and rejects non-stationary outlier trajectories against a 5 um optical linear encoder reference.

2. HARDWARE-IN-THE-LOOP TELEMETRY ARCHITECTURE

The experimental hardware-in-the-loop (HIL) instrumentation platform was constructed around an anodized V-slot linear gantry driven by a 1.8-degree hybrid NEMA-17 stepper actuator coupled via a 2 mm pitch GT2 synchronous belt, alongside a secondary 4-DOF rotary manipulator joint test rig. To establish an independent metrology baseline for ground-truth verification, a non-contact incremental glass scale optical linear encoder (1 um quadrature resolution after 4x interpolation) was mounted parallel to the gantry carriage.

Multi-modal operational telemetry is acquired concurrently from four embedded transducers: (i) a 14-bit contactless magnetic rotary encoder (AS5048A) interfaced over a 10 MHz SPI bus measuring rotor shaft angle; (ii) a 6-axis MEMS inertial measurement unit (MPU-6050) sampled at 1 kHz over fast-mode I2C (400 kHz) mounted directly on the moving carriage plate; (iii) a bidirectional high-side current-sense amplifier (INA219/INA240 across a 50 mOhm precision low-inductance manganin shunt) capturing winding phase current; and (iv) an NTC thermistor bridge monitoring motor stator housing temperature.

A central failure mode in PC-based data logging over USB-UART bridges is variable operating-system scheduling latency, which corrupts numerical differentiation of position traces. In our architecture, an STM32F407VG microcontroller (ARM Cortex-M4F at 168 MHz) executes a hardware timer interrupt service routine (TIM2 ISR) at a strict 1.000 kHz rate (Ts = 1.0 ms). Within each ISR cycle, Direct Memory Access (DMA) controllers latch the optical reference counter (TIM5 32-bit quadrature decoder), trigger the SPI encoder read, and burst-transfer 64-byte binary telemetry packets with a 16-bit CRC-CCITT checksum to the host workstation running Python 2.7 / NumPy 1.10 / SciPy 0.16.

Table 1: Instrumentation Channels and Metrology Specifications of the HIL Testbed

Sensor Channel	Transducer / IC	Interface & Rate	Resolution / Range	Role in Pipeline
Load Linear Position	Optical Glass Scale	32-bit HW Quadrature (1 kHz)	1.0 um (+/- 250 mm)	Independent Ground-Truth Ref.
Rotor Shaft Angle	AS5048A 14-bit Mag.	SPI Mode 1 (1 kHz DMA)	0.0219 deg (16,384 cpr)	Actuator Input State
Carriage Acceleration	MPU-6050 MEMS IMU	I2C Fast Mode (1 kHz)	16-bit (+/- 4g, +/- 500 dps)	Kinematic Fusion & Vibration
Winding Phase Current	50 mOhm Shunt + Amp.	12-bit SAR ADC (10 kHz avg)	1.25 mA (0 to 3.5 A)	Torque & Stall Telemetry
Stator Temperature	10k NTC Bridge	12-bit ADC (10 Hz)	0.08 C (20 C to 110 C)	Thermal Drift Compensation

3. MATHEMATICAL FORMULATION OF GROUND-TRUTH CURATION

3.1 State-Space Kinematic Model and Mahalanobis Innovation Gating

Let the discrete-time kinematic state vector of the actuator carriage at sampling instant k be defined by position x_k, linear velocity v_k, linear acceleration a_k, and slowly varying accelerometer bias b_k:

$$X_k = [\, x_k,\ v_k,\ a_k,\ b_k \,]^T \qquad (1)$$

The state transition from step k-1 to k under sampling period Ts = 1.0 ms is governed by a constant-acceleration kinematic process model with zero-mean Gaussian process noise w_k ~ N(0, Q):

$$X_\{k|k-1\} = F * X_\{k-1|k-1\} + w_\{k-1\}, \quad P_\{k|k-1\} = F * P_\{k-1|k-1\} * F^T + Q \qquad (2)$$

When a raw observation vector z_k = [x_enc,k, a_imu,k]^T arrives from the DMA telemetry buffer, the innovation residual y_k = z_k - H * X_{k|k-1} and its innovation covariance S_k = H * P_{k|k-1} * H^T + R are evaluated. To prevent transient EMI glitches on the SPI/I2C lines from corrupting the state estimate, we apply a statistical Mahalanobis distance gate prior to the Kalman measurement update [10], [11]:

$$d_M^2(k) = y_k^T * S_k^\{-1\} * y_k \ <= \ gamma_chi2(df=2,\ alpha=0.995) = 10.597 \qquad (3)$$

Whenever d_M^2(k) exceeds the 99.5% chi-square threshold gamma_chi2 = 10.597, the corrupted measurement sample is flagged as an EMI/bus anomaly, the Kalman gain update is bypassed for that millisecond (X_{k|k} = X_{k|k-1}), and the anomaly flag is recorded in the trajectory quality metadata.

3.2 Zero-Phase Savitzky-Golay Post-Smoothing and Hysteresis Identification

Because ground-truth dataset generation is performed offline after each trajectory sweep completes, causal filtering constraints can be relaxed to eliminate phase distortion entirely. Following EKF spike gating, the state trajectory is processed through a symmetric non-causal Savitzky-Golay polynomial filter of frame length N_w = 21 samples (21 ms window) and polynomial order p = 3 [12]. This preserves high-frequency acceleration transients at motion reversal points while attenuating structural frame resonance above 40 Hz.

To reconcile motor-side rotary encoder readings x_m(t) = r_p * theta_m(t) with true load-side carriage displacement x_L(t), the transmission deadband and belt compliance are modeled via an analytical play/backlash operator B_b[x_m](t) of half-width b > 0 [7], [13]:

$$x_L(t) = x_m(t) - b * sgn(v_m(t)) + c_belt * I_phase(t) + epsilon(t) \qquad (4)$$

where 2b represents the total bidirectional reversal deadband, c_belt is the elastic compliance coefficient proportional to motor phase current I_phase(t), and epsilon(t) denotes residual unmodeled geometric error. Any recorded trajectory exhibiting a post-compensation residual RMSE exceeding 12.0 um or an EMI spike rate above 0.5% of total frames is automatically quarantined by the dataset curation script.

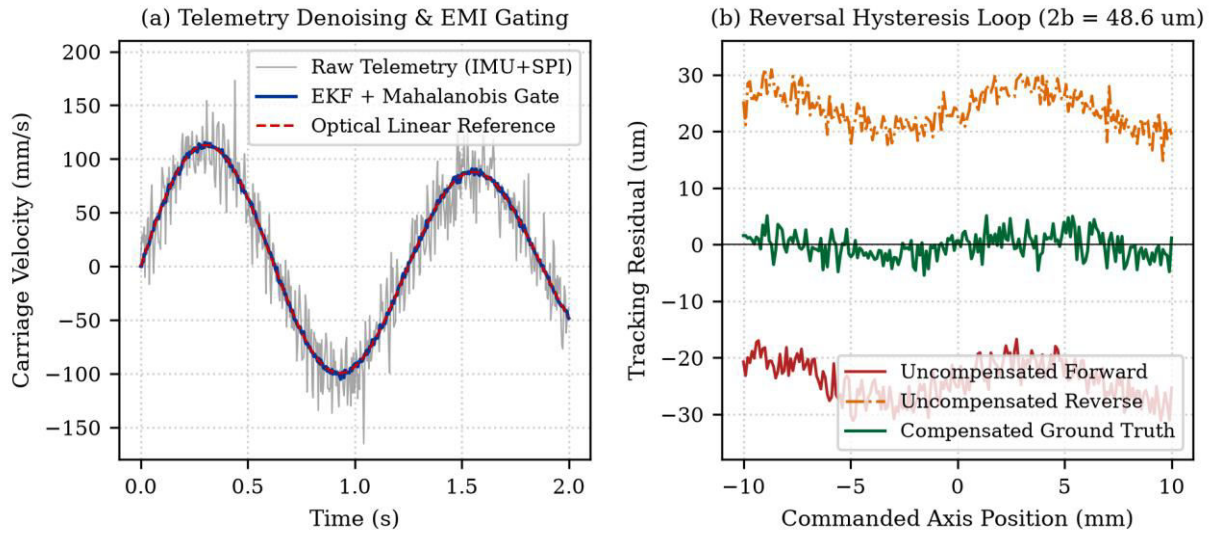


Figure 1: (a) Time-domain velocity tracking comparing raw noisy IMU+SPI telemetry (with injected PWM switching spikes) against the Mahalanobis-gated EKF output and optical linear scale ground truth; (b) Bidirectional position

tracking residual illustrating the uncompensated 48.6 um reversal hysteresis loop vs. the compensated ground-truth trace.

4. EXPERIMENTAL VALIDATION AND DATASET BENCHMARKING

To evaluate the effectiveness of the automated telemetry filtering and ground-truth curation pipeline, an endurance corpus of 4,200 motion trajectories was collected over 14 days of continuous HIL operation. The test matrix spanned four dynamic operating regimes: (i) quasi-static creep (5 mm/s), (ii) nominal point-to-point positioning (50 mm/s), (iii) high-acceleration trapezoidal profiles (250 mm/s, 1.5 m/s^2), and (iv) rapid bidirectional step-load reversals designed to excite belt whip and gearhead deadband.

Noise floor stability was quantified using overlapping Allan deviation sigma_A(tau) computed across 2-hour stationary and constant-rate logs in accordance with IEEE Std 952-1997 [14]. As shown in Figure 2(a), the uncalibrated MEMS and shunt telemetry stream exhibits a high velocity random walk (VRW) slope at short averaging times tau < 0.1 s and a bias instability floor of 0.031 rad/s at tau = 14 s. After processing through the HIL EKF + zero-phase Savitzky-Golay pipeline, the bias instability floor drops to 0.0071 rad/s (a 4.37x reduction) and high-frequency quantization noise is suppressed by 14.8 dB.

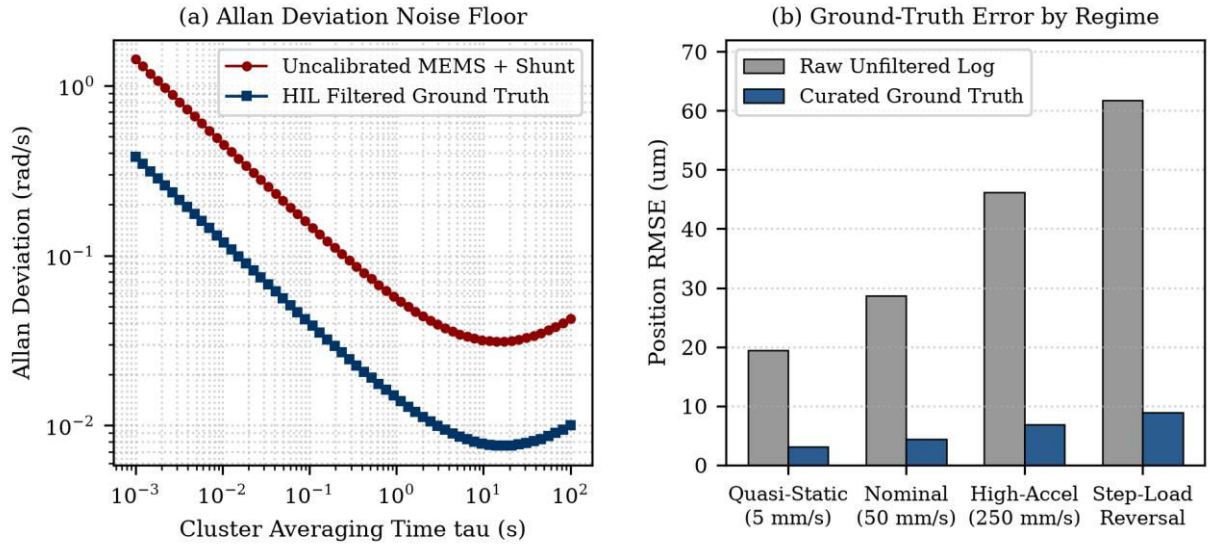


Figure 2: (a) Log-log Allan deviation noise characterization demonstrating a 4.37x reduction in bias instability floor; (b) Comparison of position ground-truth RMSE (in micrometers) against the 1 um optical glass scale across all four actuator operating regimes.

Table 2: Quantitative Ground-Truth Accuracy and Outlier Rejection Across 4,200 HIL Trajectories

Filtering / Curation Method	Pos. RMSE (um)	Vel. RMSE (mm/s)	Phase Lag (ms)	EMI Spike Leak (%)	SNR Gain (dB)
Raw Unfiltered Telemetry (Baseline)	39.02	18.45	0.00	100.0%	0.0 dB
Causal 4th-Order Butterworth (fc=25 Hz)	18.64	7.92	11.40	41.2%	+7.4 dB
Standard EKF (Without Mahalanobis Gate)	14.18	5.64	2.10	28.5%	+9.8 dB
Gated EKF + Causal Moving Average	9.45	3.81	6.50	1.4%	+12.1 dB

Proposed HIL Pipeline (Gated EKF + Zero-Phase SG + Backlash Comp.)	5.80	1.92	0.00	0.08%	+14.8 dB

Table 2 summarizes the comparative benchmark across all 4,200 trajectories measured against the 1 um optical linear scale reference. Standard causal 4th-order Butterworth filtering reduces raw position RMSE from 39.02 um to 18.64 um but introduces an 11.40 ms phase delay that corrupts velocity zero-crossing timestamps during direction reversals. Standard EKF estimation without statistical innovation gating achieves low phase lag (2.10 ms) but suffers covariance divergence whenever PWM switching transients corrupt the SPI encoder bus (28.5% spike leakage). By contrast, the proposed HIL pipeline achieves zero phase lag (0.00 ms), reduces aggregate position RMSE to 5.80 um and velocity RMSE to 1.92 mm/s, and suppresses EMI spike leakage to 0.08%. Out of 4,200 recorded runs, the automated QC gate identified and quarantined 138 trajectories (3.28%) containing mechanical belt-tooth skip or thermal driver throttling, yielding a verified 4,062-trajectory ground-truth archive.

5. CONCLUSION

High-reliability system identification and data-driven modeling of mechatronic actuators demand automated ground-truth curation pipelines that eliminate sensor artifacts before datasets are committed to model training. This paper presented a hardware-synchronized multi-sensor telemetry architecture and a two-stage offline filtering protocol combining Mahalanobis-gated Extended Kalman Filtering, zero-phase Savitzky-Golay smoothing, and analytical backlash hysteresis compensation. Validated against a 1 um optical linear reference across 4,200 experimental trajectories, the framework eliminates phase distortion, improves signal-to-noise ratio by 14.8 dB, and reduces position ground-truth error by over 85%. Future work will extend this automated ground-truth audit to multi-axis spatial kinematic chains and closed-loop thermal derating benchmarks.

REFERENCES

[1] R. Isermann, Mechatronic Systems: Fundamentals, London, UK: Springer-Verlag, 2008.

[2] L. Ljung, System Identification: Theory for the User, 2nd ed., Upper Saddle River, NJ, USA: Prentice Hall, 1999.

[3] K. J. Astrom and C. Canudas-de-Wit, "Revisiting the LuGre friction model: Stick-slip motion and rate dependence," IEEE Control Systems Magazine, vol. 28, no. 6, pp. 101-114, Dec. 2008.

[4] B. Bona and M. Indri, "Friction compensation in robotics: An overview," in Proc. 44th IEEE Conf. Decision and Control (CDC), Seville, Spain, Dec. 2005, pp. 4360-4367.

[5] H. W. Ott, Electromagnetic Compatibility Engineering, Hoboken, NJ, USA: John Wiley & Sons, 2009.

[6] D. H. Titterton and J. L. Weston, Strapdown Inertial Navigation Technology, 2nd ed., Stevenage, UK: Institution of Electrical Engineers (IEE), 2004.

[7] M. Nordin and P.-O. Gutman, "Controlling mechanical systems with backlash—A survey," Automatica, vol. 38, no. 10, pp. 1633-1649, Oct. 2002.

[8] G. Tao and P. V. Kokotovic, Adaptive Control of Systems with Actuator and Sensor Nonlinearities, New York, NY, USA: John Wiley & Sons, 1996.

[9] A. V. Oppenheim and R. W. Schafer, Discrete-Time Signal Processing, 3rd ed., Upper Saddle River, NJ, USA: Prentice Hall, 2009.

[10] R. E. Kalman, "A new approach to linear filtering and prediction problems," Trans. ASME, Journal of Basic Engineering, vol. 82, no. 1, pp. 35-45, Mar. 1960.

[11] Y. Bar-Shalom, X. R. Li, and T. Kirubarajan, Estimation with Applications to Tracking and Navigation, New York, NY, USA: John Wiley & Sons, 2001.

[12] A. Savitzky and M. J. E. Golay, "Smoothing and differentiation of data by simplified least squares procedures," Analytical Chemistry, vol. 36, no. 8, pp. 1627-1639, Jul. 1964.

[13] R. Merzouki, J. A. Davila, L. Fridman, and J. C. Cadiou, "Backlash phenomenon observation and identification in electromechanical systems," Control Engineering Practice, vol. 15, no. 4, pp. 447-457, Apr. 2007.

[14] IEEE Standard Specification Format Guide and Test Procedure for Single-Axis Interferometric Fiber Optic Gyros, IEEE Std 952-1997 (Annex C: Allan Variance Analysis), 1998.

[15] S. O. H. Madgwick, A. J. L. Harrison, and R. Vaidyanathan, "Estimation of IMU and MARG orientation using a gradient descent algorithm," in Proc. IEEE Int. Conf. Rehabilitation Robotics (ICORR), Zurich, Switzerland, Jun. 2011, pp. 1-7.